

Unsteady conjugated forced convective heat transfer in a duct with convection from the ambient

JAMES SUCEC

Department of Mechanical Engineering, University of Maine, 219 Boardman Hall,
Orono, ME 04469, U.S.A.

(Received 11 August 1986 and in final form 24 February 1987)

Abstract—A numerical finite difference solution is found for the problem of unsteady, laminar, forced convection heat transfer in a parallel plate duct with finite thermal capacity walls which interact with an ambient medium outside the duct. Response functions are presented for the duct wall temperature, fluid bulk mean temperature, and inside wall surface heat flux as a function of position down the duct and time for a range of the parameters involved. Comparisons are made with the zero thermal capacity wall solution and with quasi-steady results.

INTRODUCTION

TRANSIENT forced convection heat transfer in ducts with finite thermal energy storage capacity walls which exchange energy with an outside fluid is of importance in heat exchangers and in other engineering applications such as jet engines. Since, in most applications, the wall temperature and surface heat flux of the duct wall are not given or known *a priori*, these are heat transfer problems of a conjugated nature.

Siegel [1] develops an approximate integral method solution for the limiting case of zero thermal capacity duct wall the surface of which experiences a step change in its temperature. This corresponds to an infinite surface coefficient of heat transfer between the wall and the fluid outside of the duct. This case, with viscous dissipation included, was considered by Lin and Shih [2] who used an unsteady local similarity method which is valid at short non-dimensional distances from the duct entrance. Applications of the quasi-steady method to heat transfer in a duct with convection to an outside fluid are those of Tan and Spinner [3] for finite thermal capacity walls and of Li [4] for walls with negligible energy storage. Lin *et al.* [5] present a finite difference solution for the transient heat transfer in the zero capacity wall situation for a range of S which depends on the outside heat transfer coefficient. Steady-state forced convection in a duct communicating thermally with an outside ambient medium and including the effects of axial conduction in the walls was recently dealt with by Wijesundera [6]. An exact analytical solution, valid in the first time domain and in the transient thermal entrance region, has been found by Sucec [7] for a finite capacity wall convecting to a fluid outside the duct.

In the present work, a finite difference solution is found for the unsteady heat transfer to a fluid flowing with a laminar, fully developed velocity profile in a

parallel plate channel the finite thermal capacity walls of which transfer energy to an outside medium through a constant outside heat transfer coefficient. Results are given for the unsteady axial variation of bulk mean fluid temperature, wall temperature, and surface heat flux for a range of \hat{a} and S which are measures of the wall capacity and outside surface coefficient, respectively. The limiting 'no wall' solution is also presented and discussed as is the simpler quasi-steady solution.

ANALYSIS

Figure 1 is a depiction of the physical situation in which a fluid flowing inside the duct with a steady, laminar, fully developed velocity profile is at an initial temperature T_i when suddenly the outside of the parallel plate duct wall is exposed to an ambient fluid at temperature T_L and constant surface coefficient U . Considered are the conditions of negligible viscous dissipation and axial conduction and where the transverse resistance to heat transfer within the duct wall of thickness b is negligible. Conditions for the validity of these restrictions are discussed in ref. [11].

Under these conditions, the governing partial differential equation representing the balance of energy for the fluid inside the duct becomes

$$\frac{\partial T}{\partial t} + u(y) \frac{\partial T}{\partial x} = \alpha \frac{\partial^2 T}{\partial y^2}. \quad (1)$$

The initial and boundary conditions for the problem being considered are

$$\begin{aligned} t = 0, \quad x > 0, \quad 0 < y < R, \quad T = T_i \\ x = 0, \quad t > 0, \quad 0 < y < R, \quad T = T_i \\ y = R, \quad t > 0, \quad x > 0 \quad \partial T / \partial y = 0. \end{aligned} \quad (2)$$

Next, applying the energy balance to the duct wall

NOMENCLATURE

\hat{a}	ratio of thermal energy storage capacity of inside fluid to that of the duct wall, $\rho c_p R / \rho_w c_{p_w} b$	$\Delta t, \Delta x, \Delta y$	finite difference increment sizes in t, x and y
A	constant in equation (18)	T	temperature at any position and time
b	thickness of duct wall	T_i	initial temperature as well as inlet fluid temperature
B	constant in equation (18)	T_L	temperature of ambient outside of duct
\mathbf{B}	matrix defined by equation (10)	u, u_m	local and mass average fluid velocity, respectively
c_p, c_{p_w}	specific heats of fluid and duct wall, respectively	U	heat transmission coefficient between ambient and duct wall
c_1	function of the Prandtl number in equation (18)	x	space coordinate along duct
Δc_j	$u_j \Delta t / \Delta x$	X	$\alpha x / R^2 u_m$
\mathbf{C}	square diagonal matrix defined by equation (10)	y	space coordinate normal to duct wall
F	Fourier number, $\alpha t / R^2$	Y	y / R
ΔF	$\alpha \Delta t / \Delta y^2$		
h	heat transfer coefficient used in the quasi-steady analysis		
i, j	indices locating nodes in the x - and y -directions, respectively		
k	thermal conductivity of inside fluid (when used as a superscript, index which fixes time)		
Nu	Nusselt number for quasi-steady analysis, hR/k		
q	heat flux at inside surface of duct wall		
Q_w	dimensionless heat flux, $qR/k(T_L - T_i)$		
R	half height of parallel plate channel		
ΔR	$\hat{a} \alpha \Delta t / R \Delta y$		
S	UR/k		
ΔS	$\hat{a} S \alpha \Delta t / R^2$		
t	time		

Greek symbols

α	thermal diffusivity of inside fluid
β_1	function of the Prandtl number in equation (18)
ρ, ρ_w	mass density of inside fluid and duct wall, respectively
τ	non-dimensional time used in equation (18)
ϕ	$[T(x, y, t) - T_i] / (T_L - T_i)$
ϕ_B, ϕ_w	bulk mean fluid and wall value of ϕ , respectively
ϕ_d	difference between exact and quasi-steady solution, $\phi - \phi_q$
ϕ_i^k	single column matrix of ϕ values of the nodes in the y -direction at a value of x and t .

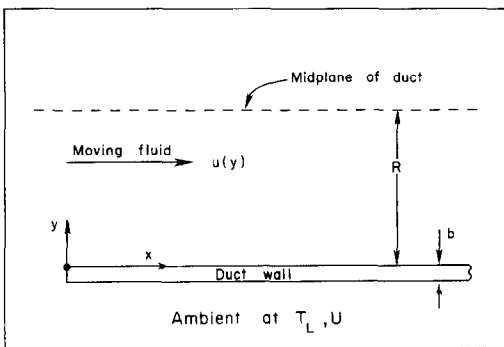


FIG. 1. Schematic of parallel plate duct.

yields, after invoking the conjugation conditions of flux and temperature continuity at $y = 0$, the following equation:

$$y = 0, \quad x > 0, \quad t > 0, \quad U(T_L - T) = -k \left(\frac{\partial T}{\partial y} \right)_{y=0} + \rho_w c_{p_w} b \frac{\partial T}{\partial t}. \quad (3)$$

We now introduce non-dimensional variables and parameters, namely,

$$\phi = [T(x, y, t) - T_i] / (T_L - T_i),$$

$$F = \alpha t / R^2,$$

$$X = \alpha x / R^2 u_m,$$

$$Y = y / R,$$

$$S = UR/k,$$

and

$$\hat{a} = \rho c_p R / \rho_w c_{p_w} b.$$

With these and the use of the velocity profile, the non-dimensional mathematical problem statement becomes

$$\frac{\partial \phi}{\partial F} + 3[Y - Y^2/2] \frac{\partial \phi}{\partial X} = \frac{\partial^2 \phi}{\partial Y^2} \quad (4)$$

$$\begin{aligned} F = 0, \quad X > 0, \quad 0 < Y < 1 \quad \phi = 0 \\ X = 0, \quad F > 0, \quad 0 < Y < 1 \quad \phi = 0 \\ Y = 1, \quad F > 0, \quad X > 0 \quad \partial \phi / \partial Y = 0. \end{aligned} \quad (5)$$

$$Y = 0, \quad X > 0, \quad F > 0 \quad S(1 - \phi) = -\frac{\partial \phi}{\partial Y} + \frac{1}{\hat{a}} \frac{\partial \phi}{\partial F}. \quad (6)$$

Finite difference equations

Energy balances on small, but finite, volumes of the fluid flowing inside the duct and on the duct wall were used to develop the following implicit set of finite difference equations:

$$j = 1 \quad [1 + \Delta R + \Delta S]\phi_{i,1}^{k+1} - \Delta R\phi_{i,2}^{k+1} = \phi_{i,1}^k + \Delta S \quad (7)$$

$$2 \leq j \leq N-1 \quad -\Delta F\phi_{i,j-1}^{k+1} + [2\Delta F + \Delta c_j + 1]\phi_{i,j}^{k+1} - \Delta F\phi_{i,j+1}^{k+1} = \phi_{i,j}^k + \Delta c_j\phi_{i-1,j}^{k+1} \quad (8)$$

$$j = N \quad -2\Delta F\phi_{i,N-1}^{k+1} + [2\Delta F + \Delta c_N + 1]\phi_{i,N}^{k+1} = \phi_{i,N}^k + \Delta c_N\phi_{i-1,N}^{k+1} \quad (9)$$

where

$$\Delta S = \hat{a}S\alpha\Delta t/R^2,$$

$$\Delta R = \hat{a}\alpha\Delta t/R\Delta y,$$

$$\Delta F = \alpha\Delta t/\Delta y^2,$$

$$\Delta c_j = u_j\Delta t/\Delta x.$$

The consistency of the finite difference equations (7)–(9) with the partial differential equations and mid-channel boundary condition, equations (4), (6), and the last of (5), was demonstrated by the appropriate Taylor expansions which give the truncation error as $O(\Delta x) + O(\Delta y) + O(\Delta t)$.

In order to investigate stability of the finite difference equations by the Matrix method, the difference equations (7)–(9) are rewritten as the following matrix equation:

$$\phi_i^{k+1} = \mathbf{B}^{-1}\mathbf{C}\phi_{i-1}^{k+1} + \mathbf{B}^{-1}\phi_i^k. \quad (10)$$

The stability of the set of finite difference equations given in equation (10) is related to the boundedness of the matrices $\mathbf{B}^{-1}\mathbf{C}$ and \mathbf{B}^{-1} (see Richtmyer and Morton [8]). Since these are not symmetric matrices, the spectral radius condition may not be an adequate representation of the norm of these matrices and hence instead, it was required that the ‘infinite’ or ‘maximum’ norm be less than or equal to unity (see Mitchell [9]). Study of the infinite norms led to the conclusion that the norm of both the above matrices satisfies the inequality unconditionally. Hence, the finite difference equations exhibit unconditional stability.

Lattice refinement studies revealed the points at which the solution of the finite difference equation became independent of the various increment sizes in X , Y and F . The final increment sizes used depended upon the case being solved and on the X and F values of interest. The maximum number of nodes needed across the half height R of the duct was 193 with usually 97 or 49 sufficing, whereas the smallest ΔX needed was 0.0004 and the smallest value of $\alpha\Delta t/R^2$ required 0.000625.

Some checks of the finite difference predictions vs available analytical solutions were also made. For the pure conduction phase of the transient caused by a step change in the wall temperature, the finite difference calculations were compared to the exact analytical solution as given in Siegel [1] and agreement within a fraction of a percent was noted for the range of F between 0.01 and 1.0. However, a value of $\alpha\Delta t/R^2 = 0.0000625$ was required to achieve agreement of 0.25% at the lowest F , $F = 0.01$, for the surface heat flux. This also explains the large discrepancy between the exact and finite difference solutions at $F = 0.01$ in the results of Lin *et al.* [5] where their predicted flux is in error by about 70% due to the use of too large a time increment, namely $\alpha\Delta t/R^2 = 0.01$, at this low value of F . The finite difference program was also run to the steady state for the case of an isothermal wall and contrasted with the exact analytical solution for this condition as given in Kays and Crawford [10]. Complete agreement was found for $0.01 < X < \infty$. A final steady-state check was made by comparing the finite difference calculations for steady-state heat transfer between the duct and the ambient for $S = 1.0$ with the analytical predictions given by Wijesundera [6]. The comparison was made for the lowest value of the wall axial conduction parameter, namely 10^{-4} , which he reports. For values of $X > 0.2$, where the Nusselt number is essentially independent of the wall conduction parameter, the agreement between the finite difference results and those of ref. [6] is complete. For lower values of X , the results of ref. [6] indicate an increasing dependence on the wall conduction parameter and so the present finite difference results gradually deviate from those of ref. [6] giving a difference of about 3% at $X = 0.01$.

Quasi-steady analysis

In this simplest approach to unsteady convection problems, use is made of a constant surface coefficient of heat transfer, h , between the wall and the inside fluid. This constant h value is generally chosen as the one for fully developed flow past an isothermal wall under steady-state conditions. Energy balances on the wall and fluid yield the governing equations as follows:

$$\frac{1}{\hat{a}} \frac{\partial \phi_w}{\partial F} + Nu(\phi_w - \phi_B) = S(1 - \phi_w) \quad (11)$$

$$\frac{\partial \phi_B}{\partial F} + \frac{\partial \phi_B}{\partial X} = Nu(\phi_w - \phi_B). \quad (12)$$

Solving equations (11) and (12) by Laplace transformations for the limiting case of negligible energy storage capacity of the wall relative to that of the inside fluid, $\hat{a} \rightarrow \infty$, the ‘no-wall’ condition, yields

$$\phi_w = 1 - \left(\frac{Nu}{Nu + S} \right) e^{-NuSF/(Nu+S)} \quad \text{for } F < X \quad (13)$$

$$\phi_w = 1 - \left(\frac{Nu}{Nu+S} \right) e^{-NuSX/(Nu+S)} \quad \text{for } F > X. \quad (14)$$

Equation (11) yields the bulk mean temperature as being

$$\phi_B(F, X) = \left(\frac{Nu+S}{Nu} \right) \phi_w(F, X) - \frac{S}{Nu}. \quad (15)$$

The quasi-steady solution for the more general case where \hat{a} is finite is given in Sucec [7] for the first time domain, $F < X$.

To investigate conditions under which one would expect the quasi-steady results to give predictions of high accuracy, the procedure advanced in Sucec [11] was applied to the present problem, and leads to the following conclusions relative to the accuracy of the quasi-steady solution as $\hat{a} \rightarrow \infty$. ϕ_d is the difference between the exact solution and the quasi-steady solution

$$\begin{aligned} \phi_d &\rightarrow 0 \quad \text{as } S \rightarrow 0 \quad \text{for all } X, Y, F \\ \phi_d &\rightarrow 0 \quad \text{as } F \rightarrow \infty, \quad \text{all } S, Y, X \quad \text{when } F < X \end{aligned} \quad (16)$$

$$\phi_d \rightarrow 0 \quad \text{as } X \rightarrow \infty, \quad \text{all } S, Y, F \quad \text{when } F > X.$$

In addition it was found that ϕ_d is not expected to approach zero either as $X \rightarrow 0$ or as $F \rightarrow 0$. Consideration of the quasi-steady solution function for ϕ_w given in ref. [7] for finite \hat{a} yields the condition that

$$\phi_d \rightarrow 0 \quad \text{as } \hat{a} \rightarrow 0 \quad \text{for all } X, Y, F. \quad (17)$$

These conditions, (16) and (17), for expected good accuracy from the quasi-steady solution, will be discussed and commented on further in the next section.

RESULTS AND DISCUSSION

Response curves plotted from the finite difference solution are presented in Figs. 2-9 for the wall temperature, ϕ_w , fluid bulk mean temperature, ϕ_B , and heat flux to the inside fluid, Q_w . The parameter values are $\hat{a} = 0.10, 1.0, 10.0$, and ∞ for the storage capacity ratio of the inside fluid to the duct wall, and $S = 2.0$ and 10.0 for the dimensionless outside surface coefficient.

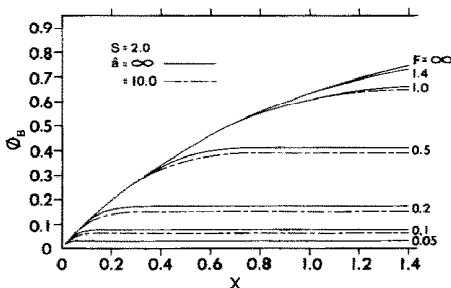


FIG. 2. Axial and timewise variation of bulk mean fluid temperature.

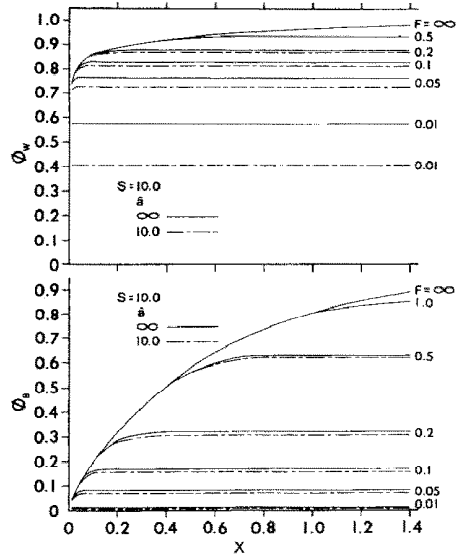


FIG. 3. Axial and timewise variation of wall temperature and fluid bulk mean temperature.

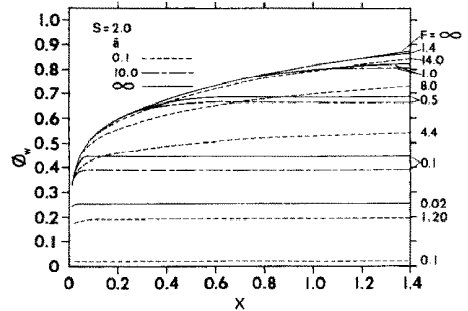


FIG. 4. Axial and timewise variation of wall temperature.

First, we compare the results for the limiting case of negligible thermal energy storage capacity of the wall relative to the fluid, $\hat{a} \rightarrow \infty$, the 'no wall' solution, to the case of a relatively large finite value of $\hat{a} = 10.0$. As is evident by an examination of the curves in Figs. 2-6, how closely the results for $\hat{a} = 10.0$ are represented by the limiting case of $\hat{a} \rightarrow \infty$ depends upon time, F , the value of S , and upon whether one is dealing with ϕ_w , ϕ_B or Q_w . For $S = 10.0$, the limiting solution for $\hat{a} \rightarrow \infty$ would be a good approximation for $\hat{a} \geq 10.0$ as long as $F > 0.20$ whereas the same degree of approximation for $S = 2.00$ would require F values in excess of $F = 0.50$. This trend of increasing agreement between finite \hat{a} solutions and the $\hat{a} \rightarrow \infty$ solution as S increases is readily explained on a physical basis as follows. As S gets larger, the transient initiated by the sudden change in the ambient temperature from T_i to T_L comes closer to a step change in the wall temperature and reaches this condition as $S \rightarrow \infty$ for the case considered of negligible temperature drop across the duct wall. If the wall temperature is practically step changed to a near constant value of T_L , it is then immaterial what the wall thermal

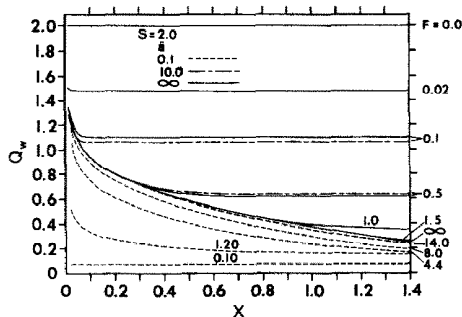


FIG. 5. Axial and timewise variation of heat flux at inside surface.

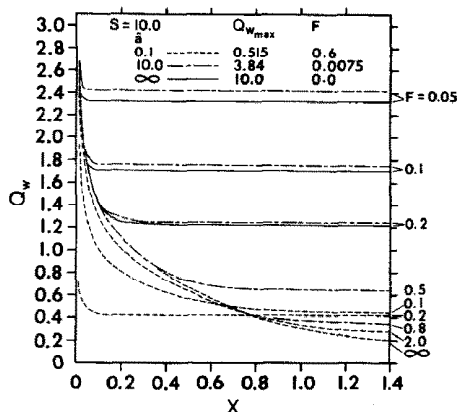


FIG. 6. Axial and timewise variation of heat flux at inside surface. $Q_{w,max}$ occurs for $X \geq 2.0, 0.0125,$ and 0.0 for $\hat{a} = 0.1, 10.0,$ and $\infty,$ respectively.

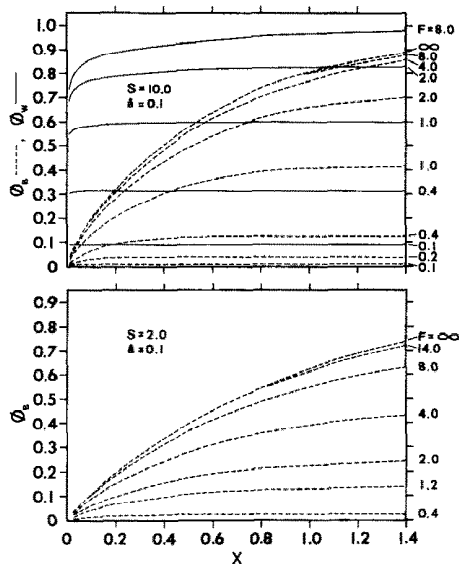


FIG. 7. Axial and timewise variation of wall temperature and fluid bulk mean temperature.

capacity is since it behaves the same as if it had no thermal capacity.

Where the curves for $\hat{a} = 10.0$ and $\hat{a} \rightarrow \infty$ virtually coincide in the figures, such as for $F \geq 0.50$ in Fig. 6, only a single curve is shown which represents both values of \hat{a} .

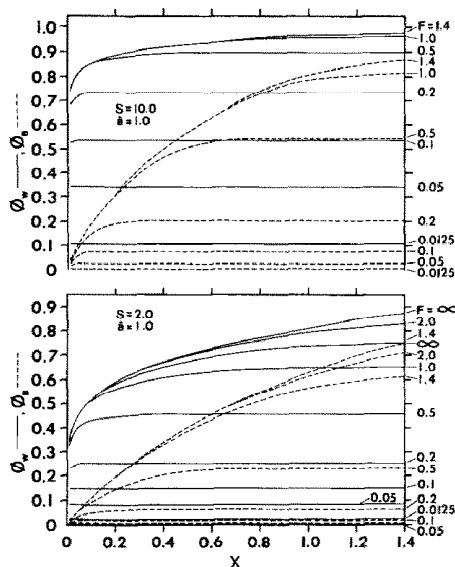


FIG. 8. Axial and timewise variation of wall temperature and fluid bulk mean temperature.

Next, looking at the qualitative trends in Figs. 2-4, 7 and 8 for the wall and bulk mean temperature, ϕ_w and ϕ_b , for $\hat{a} = 0.1, 1.0, 10.0$ and ∞ , it is seen that both ϕ_w and ϕ_b increase monotonically to their eventual state distributions in X for all values of \hat{a} and S with $\hat{a} \rightarrow \infty$ yielding the fastest transient and, because of the relatively large wall thermal capacity, $\hat{a} = 0.10$ giving the slowest transient. For example, in Fig. 4, the steady-state wall temperature distribution has been essentially reached at all $X < 1.4$ at $F = 1.40$ when $\hat{a} \rightarrow \infty$, while for $\hat{a} = 0.10$ this same steady-state distribution has not yet been reached even at $F = 14.0$. For a fixed value of \hat{a} , the largest S value gives the fastest transient because of the decreased thermal resistance between the outside fluid and duct wall.

The most significant differences in behavior between the $\hat{a} \rightarrow \infty$ and any case of finite \hat{a} occur for the non-dimensional surface heat flux, Q_w , presented in Figs. 5, 6 and 9. Q_w is also the function which exhibits the most complex dependency on time F and distance X , at least for finite values of \hat{a} . One first observes that for $\hat{a} \rightarrow \infty$, Q_w experiences a step increase to its maximum value right at $F = 0$ and then monotonically decreases to its eventual steady-state distribution at every X . On the other hand, for all finite values of \hat{a} , $Q_w = 0$ at $F = 0$ and then exhibits a quite complicated behavior after that. The reason for this quite different value of Q_w at $F = 0$ is contained in the energy balance on the wall, equation (6). Here it is seen that as $\hat{a} \rightarrow \infty$, the last term vanishes and $-\left[\partial\phi/\partial Y\right]_{Y=0} = S[1 - \phi_w]$. At $F = 0$, $\phi_w = 0$ thus giving the flux its maximum value. For a finite \hat{a} , however, the last term in equation (6) does not vanish and in fact exactly balances the $S[1 - \phi_w]$ at $F = 0$ so that the flux is zero. This has been verified analytically as well by recourse to the analytical solution for the flux presented in ref. [7] which is valid at short times in the transient thermal

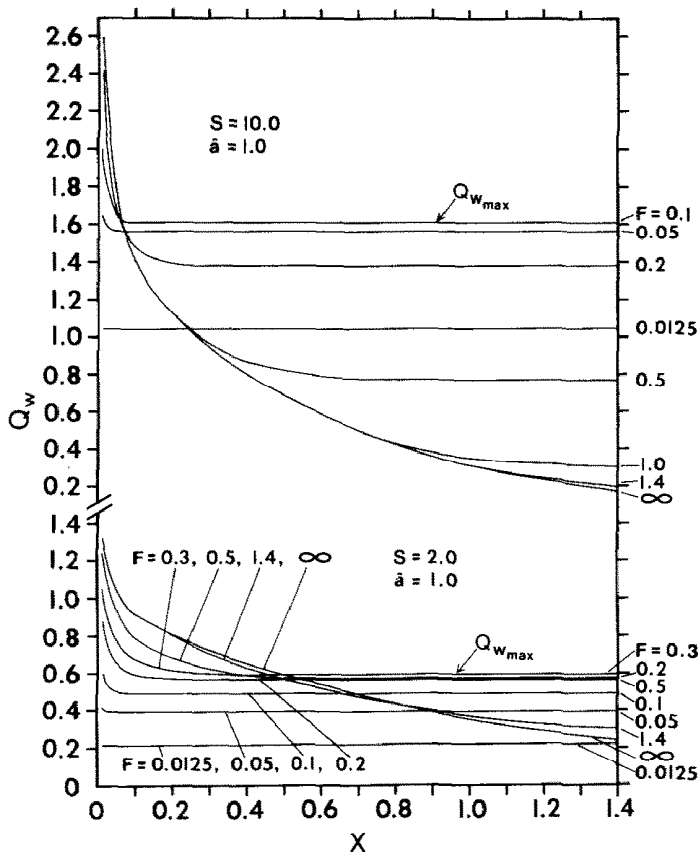


FIG. 9. Axial and timewise variation of heat flux at inside surface.

entrance region, two conditions which are satisfied everywhere as $F \rightarrow 0$. Looking now at the case of $\hat{a} = 1.0$ and $S = 2.0$ in Fig. 9, when $X = 0.7$, it is seen that Q_w increases from its initial value of zero and reaches a maximum at some value of F beyond 0.2 (the detailed numerical finite difference results indicate that $(Q_w)_{\max} = 0.60$ at $F = 0.30$) and then starts decreasing toward its eventual steady-state value. But, as also can be detected on the figure by looking at the relative positions of the curves at $F = 0.5, 1.4$, and the steady state for $X = 0.7$, the numerical results indicate that Q_w decreases below the steady state to a value of 0.4738 at $F = 1.3$ and then increases toward the steady-state value of about 0.484 at $F \approx 2.5$. An even greater magnitude of this effect of dropping below the steady-state flux and then approaching it from below occurs at $X = 0.5$. Here Q_w drops below the steady state to a value of 0.56 at $F = 0.8$ and gradually rises to the steady-state value of $Q = 0.591$ at $F = 2.5$. This phenomenon occurs in the second time domain, $F > (2/3)X$, that is, for times greater than the time, $(2/3)X$, needed for the fastest moving fluid particle which was at the duct entrance at $F = 0$ to reach the X location of interest. The effect is caused by the interaction between the conduction heat transfer mode in the Y -direction and the energy being transported by convective effects, the velocity field, in the X -direction, as they approach the balance between

them which causes the storage term, $\partial\phi/\partial F$, to be zero in the steady state. This particular effect was also seen in some of the much earlier work on unsteady convection involving non-conjugated problems which had a step change in surface temperature. In the work on unsteady free convection by Siegel [12], this effect was noted and in another analysis of unsteady combined free and forced convection by Zeiberg and Mueller [13], an oscillatory approach of the flux to the final steady state was predicted. Analytical support for this phenomenon is available in Riley [14] where unsteady forced convection over a flat plate, when a step change in surface temperature occurs, is considered. Riley derives a result, his equation (64), for the dominant term for the heat flux q as it approaches the steady state and this expression can be written as

$$q \sim B - A\tau^{1+c_1} \exp[-\beta_1\tau^2/3] \quad (18)$$

where B and A are positive constants while c_1 and β_1 both depend inversely on the Prandtl number. Although not pointed out in ref. [14], a little analysis of equation (18) shows that q drops below the steady-state value and then gradually approaches it from below, the same behavior predicted by the finite difference solution of the present work.

Study of Figs. 2-9 lead to the following trends with the non-dimensional heat transfer parameter S .

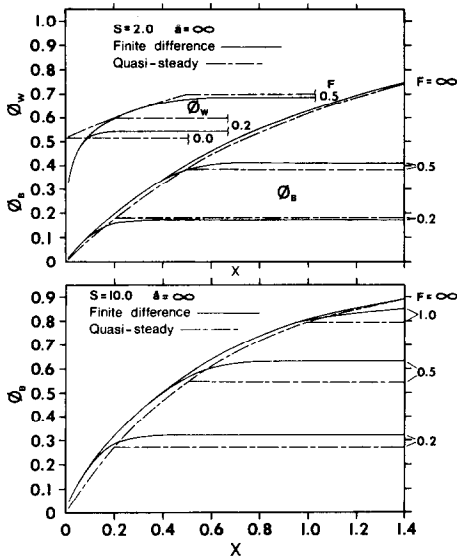


FIG. 10. Comparison of finite differences and quasi-steady predictions of the wall temperature and fluid bulk mean temperature.

Higher values of S lead to higher values of both ϕ_w and ϕ_B for all \hat{a} , F and X . The flux, Q_w , however, exhibits a more complex dependency upon S . At lower values of time, F , Q_w is greater at higher values of S than it is for lower S values. At larger F , and to the steady state, Q_w is greater at lower X for the higher S , but is lower for higher S at the larger X values. This last observation is explained by realizing that near the steady state, all values of S for long enough ducts eventually raise ϕ_B and ϕ_w to the limit 1.0. Thus, comparing equal length ducts for different S values, it is apparent that a higher S gives ϕ_B closer to 1 near the downstream end than do the smaller S values. Hence, the flux must be lower in the downstream portion of ducts when S is large, since long enough ducts for any S lead to very low flux values near the end.

Lastly, Fig. 10 gives some comparisons between the quasi-steady solution function for ϕ_w and ϕ_B , equations (13)–(15), and the finite difference results for the limiting case of $\hat{a} \rightarrow \infty$. The results in the figure are indicative of, in general, the fairly large differences between the simple quasi-steady predictions of the dashed curves and the finite difference solution plotted as the solid lines. It is seen that for the bulk mean temperature, ϕ_B , the error in the quasi-steady solution first increases with time and then decreases, whereas the error in the wall temperature is a maximum at $F = 0$ and then continually decreases. This behavior occurs because the quasi-steady solution cannot satisfy the initial condition at the wall because of the finite value of Nu used in equation (11) along with $\hat{a} \rightarrow \infty$. Thus, from equation (13) at $F = 0$, the quasi-steady value of ϕ_w at $F = 0$ is $\phi_w = S/(Nu + S)$ rather than the actual value of zero. However, the quasi-steady solution for ϕ_B , in equation (15), is able to

satisfy the condition that $\phi_B = 0$ at $F = 0$ and so causes the error in the value of ϕ_B to increase and then eventually decrease for the quasi-steady result. It can also be noticed, in the results plotted for $S = 2.0$ in Fig. 10, that the value of ϕ_B predicted by the quasi-steady solution initially is larger than the finite difference result and then becomes smaller than the correct result for ϕ_B , the finite difference result. This behavior is caused by the fact that in the quasi-steady solution, ϕ_w starts at $S/(Nu + S)$ instead of zero and thus, even with the small value of Nu used, the heat flux is initially greater than the actual flux leading to values of ϕ_B greater than the actual values. As some time passes, however, the much larger transient Nusselt numbers implied by the finite difference solution quickly cause the quasi-steady ϕ_B to be below the true values. Next, the general trends, exhibited by the results plotted in Fig. 10, which lead to good agreement between the quasi-steady and the finite difference solution are examined. As F gets large in time domain I, $F < (2/3)X$, the quasi-steady results get closer to the correct results. This is most easily seen by reference to the wall temperature results for $S = 2.0$. Upon comparison of the results for $S = 10.0$ to those for $S = 2.0$, we see that as S gets smaller, the quasi-steady predictions get better. Also, in the second time domain, $F > (2/3)X$, as $X \rightarrow \infty$, the quasi-steady predictions become very good. All three of these trends regarding the accuracy of the quasi-steady results are the ones predicted by the analysis which led to equation (16). The other conclusions, just after equation (16), with regard to the behavior as $X \rightarrow 0$ or as $F \rightarrow 0$, are also confirmed by the results in Fig. 10.

Perhaps also worth mentioning is the fact that a proper assessment of the quality of a quasi-steady solution in conjugated problems, or even non-conjugated duct flow situations, cannot rest upon a comparison of the quasi-steady vs the true Nusselt number alone. In these problems one is primarily trying to predict ϕ_B and ϕ_w in a conjugate duct flow or ϕ_B in a non-conjugated duct flow situation and the Nusselt number error is not a direct measure of the error in ϕ_B and ϕ_w . The Nusselt number is a connection among ϕ_B , ϕ_w and Q_w in such a problem, yet ref. [5] alludes to it as the sole criterion of quasi-steady accuracy. The present results include situations where it was found that the Nusselt number error greatly exceeded the error in either ϕ_B or ϕ_w for the quasi-steady solution.

CONCLUSION

A finite difference solution is developed for the unsteady forced convection situation where a fluid flowing inside a duct with finite thermal capacity walls is subject to a step change in the temperature of an ambient medium outside the duct. Differences between the limiting ‘no-wall’ solution, $\hat{a} \rightarrow \infty$, and the solution for finite capacity walls, \hat{a} finite, are noted

and discussed. It is seen that the finite \hat{a} solutions are slower transients in the wall temperature, bulk mean fluid temperature, and wall heat flux than is the case for the limiting solution of $\hat{a} \rightarrow \infty$.

The results indicate that fairly large values of \hat{a} are needed, certainly in excess of $\hat{a} = 10.0$, in order that the solution for $\hat{a} \rightarrow \infty$ serve as an adequate approximation for finite \hat{a} for small enough values of non-dimensional time F .

Noted also is the complexity of the surface heat flux behavior for finite \hat{a} with Q_w rising from zero to a maximum value, then decreasing beyond the steady-state flux followed by a final rise to the steady state.

Comparison of the finite difference results with those of a quasi-steady analysis indicated that fairly large errors could result from the quasi-steady solution.

An analysis was carried out to determine the conditions under which one would expect the quasi-steady results to approach the true solution to the problem. The analysis indicated that coalescence of the two results would occur as S gets small; as \hat{a} becomes smaller; as F gets larger in the first time domain; or as X gets larger in the second time domain. The comparison of the numerical results verified these predicted conditions.

REFERENCES

1. R. Siegel, Heat transfer for laminar flow in ducts with arbitrary time variations in wall temperature, *Trans. Am. Soc. Mech. Engrs J. Appl. Mech.* **27**, 241–249 (1960).
2. H. T. Lin and Y. P. Shih, Unsteady thermal entrance heat transfer of power law fluids in pipes and plate slits, *Int. J. Heat Mass Transfer* **24**, 1531–1539 (1981).
3. K. S. Tan and I. H. Spinner, Dynamics of a shell and tube heat exchanger with finite tube wall heat capacity and finite shell side resistance, *Ind. Engng Chem. Fundam.* **17**(4), 353–358 (1978).
4. C.-H. Li, Exact transient solutions of parallel current transfer processes, *Trans. Am. Soc. Mech. Engrs J. Heat Transfer* **108**(2), 365–369 (1986).
5. T. F. Lin, K. H. Hawks and W. Leidenfrost, Unsteady thermal entrance heat transfer in laminar pipe flows with step change in ambient temperature, *Warme- und Stoffübertragung* **17**, 125–132 (1983).
6. N. E. Wijesundera, Laminar forced convection in circular and flat ducts with wall axial conduction and external convection, *Int. J. Heat Mass Transfer* **29**, 797–807 (1986).
7. J. Sucec, Exact solution for unsteady conjugated heat transfer in the thermal entrance region of a duct, A.S.M.E. Paper No. 85-WA/HT-71 (1985). Also to appear in *Trans. Am. Soc. Mech. Engrs J. Heat Transfer*.
8. R. D. Richtmyer and K. W. Morton, *Difference Methods for Initial Value Problems*, 2nd Edn. Wiley, New York (1967).
9. A. R. Mitchell, *Computational Methods in Partial Differential Equations*. Wiley, London (1976).
10. W. M. Kays and M. E. Crawford, *Convective Heat and Mass Transfer*, 2nd Edn. McGraw-Hill, New York (1980).
11. J. Sucec, Transient heat transfer between a plate and a fluid whose temperature varies periodically with time, *Trans. Am. Soc. Mech. Engrs J. Heat Transfer* **102**(1), 126–131 (1980).
12. R. Siegel, Transient free convection from a vertical flat plate, *Trans. Am. Soc. Mech. Engrs* **80**, 347–359 (1958).
13. S. L. Zeiberg and W. K. Mueller, Transient laminar combined free and forced convection in a duct, *Trans. Am. Soc. Mech. Engrs J. Heat Transfer* **84**(2), 141–148 (1962).
14. N. Riley, Unsteady heat transfer for flow over a flat plate, *J. Fluid Mech.* **17**(1), 97–104 (1963).

CONVECTION THERMIQUE VARIABLE, COUPLEE, FORCEE DANS UN CANAL AVEC CONVECTION A L'AMBIANCE

Résumé—Une résolution numérique aux différences finies est appliquée au problème de la convection thermique variable, laminaire, dans un canal à plans parallèles, avec des parois à capacité thermique finie qui sont soumises à l'ambiance externe au canal. On présente des réponses pour la température des parois, la température moyenne du fluide, et pour le flux thermique dans la paroi en fonction de la position et du temps, pour un domaine considéré des paramètres. Des comparaisons sont faites avec la solution pour des parois à capacité nulle et avec des résultats de régime quasi-permanent.

GEKOPPELTER, INSTATIONÄRER WÄRMEAUSTAUSCH DURCH ERZWUNGENE KONVEKTION IN EINEM KANAL MIT KONVEKTIVER VERBINDUNG ZUR UMGEBUNG

Zusammenfassung—Für das Problem der instationären Wärmeübertragung durch laminare, erzwungene Konvektion in einem, von parallelen Platten gebildete Kanal wurde eine numerische Lösung nach dem Verfahren der Finiten-Differenzen gefunden. Die Wände des Kanals besitzen eine endliche Wärmekapazität und stellen den thermischen Kontakt mit dem, den Kanal umgebenden Medium her. Für einen gewissen Parameterbereich werden die zeitlichen Verläufe und die Verläufe in Kanal-Längsrichtung für folgende Größen angegeben: Temperatur der Kanalwand, mittlere Fluidtemperatur im Kanal und Wärmestromdichte an der inneren Kanalwand. Die Ergebnisse der quasi-stationären Betrachtung und der Lösung des Spezialfalls, in welchem die Wand keine Wärmekapazität besitzt, wurden mit den Ergebnissen dieser Untersuchung verglichen.

НЕСТАЦИОНАРНЫЙ СОПРЯЖЕННЫЙ КОНВЕКТИВНЫЙ ПЕРЕНОС ТЕПЛА В КАНАЛЕ С УЧЕТОМ ВОЗДЕЙСТВИЯ ВНЕШНЕЙ СРЕДЫ

Аннотация—Численно конечно-разностным методом решена задача о нестационарном переносе тепла при вынужденной ламинарной конвекции в канале, образованном параллельными пластинами конечной теплоемкости с учетом влияния внешней среды. Представлены распределения температуры стенок канала, средне-объемной температуры жидкости и теплового потока на внутренней поверхности стенки в зависимости от расстояния вдоль канала и времени и для определенного диапазона параметров. Проведено сравнение с решением при нулевой теплоемкости стенок и квазистационарном режиме.